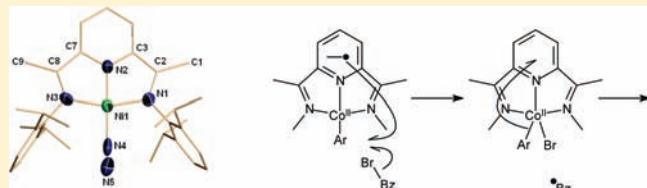


Redox-Active Ligands and Organic Radical Chemistry

Di Zhu,[†] Indira Thapa,[‡] Ilia Korobkov,[‡] Sandro Gambarotta,^{*,‡} and Peter H. M. Budzelaar^{*,†}[†]Department of Chemistry, University of Manitoba, Winnipeg, Manitoba R3T 2N2, Canada[‡]Department of Chemistry, University of Ottawa, Ottawa, Ontario K1N 6N5, Canada

S Supporting Information

ABSTRACT: Knowledge about bonding in diiminepyridine (L) halide, alkyl, and dinitrogen complexes of the metals iron, cobalt, and nickel is summarized, and two new examples are added to the set: $L^1Ni(Me)$ and $L^1Ni(N_2)$. Reactivity of these types of complexes is discussed in terms of organic radical chemistry. New C–C couplings with L^2CoAr complexes are described and proposed to involve halide abstraction and radical coupling. Calculations support the high tendency of the diiminepyridine ligand to accept an electron coming from a metal–carbon bond and so facilitate loss of a radical.



INTRODUCTION

Conjugated C–N ligands like α -diimines (DIM), iminepyridines (IMPY), bipyridines, terpyridines, and, in particular, 2,6-diiminepyridines (DIMPY)^{1,2} (Scheme 1) have long been recognized as “non-innocent”. Their π systems can easily accept one or more electrons, leading to the formation of stable complexes, where the metal has a deceptively low *formal* oxidation state, while the actual electronic structure is best viewed as containing a higher-valent metal bound to a negatively charged ligand (“electronic non-innocence”).^{2–11} The same ligands (at least the imine-containing DIM, IMPY, and DIMPY) also have a tendency to become involved in chemical reactions (“chemical non-innocence”), with the most important one being alkylation at various positions of the ligand skeleton (DIM,^{3,11–19} IMPY,^{3,17,20,21} and DIMPY^{22–29}). It seems reasonable to assume that these two properties are somehow connected,³⁰ although limited evidence for this has been provided so far for DIMPY ligands.³¹ In the present paper, we will summarize what is known about the bonding and electronic structures of DIMPY complexes of iron, cobalt, and nickel halides, alkyls, and dinitrogen complexes, then discuss some of the reactivities of these complexes, and finally try to link electronic and chemical noninnocence with each other and with the reactivities of the complexes.

The “standard” DIMPY ligand (L^1 , Scheme 2) has methyl groups at the imine carbon atoms and 2,6-diisopropylphenyl groups at the imine nitrogen atoms. In addition, we will in this paper regularly refer to the somewhat less bulky ligand L^2 with 2,6-dimethylphenyl groups at the nitrogen atom. Other ligands will be denoted more explicitly as $L(R,Ar)$ where necessary; the symbol L indicates a generic diiminepyridine ligand.

ELECTRONIC STRUCTURE OF METAL HALIDES AND METAL ALKYLs

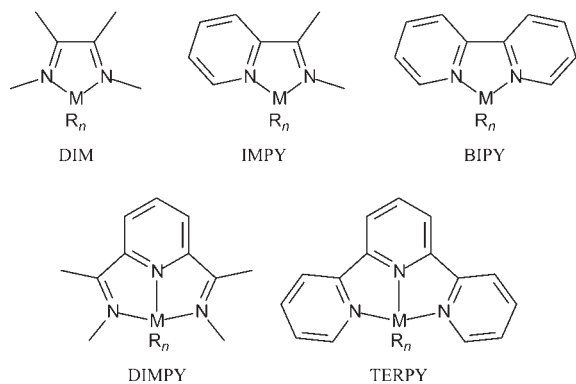
Complexes LMX_2 ($M = Fe, Co, Ni$; $X = \text{halide}$) are all high-spin and contain a neutral (“innocent”) ligand L^0 and a truly divalent

metal center.²⁸ The reduction of high-spin ($S = 2$) $LFeX_2$ to $LFeX$ is ligand-centered, and the resulting complexes have a ligand radical anion L^- ($S = 1/2$) antiferromagnetically coupled to high-spin Fe^{II} ($S = 2$), leading to a final $S = 3/2$ ground state.³² The $C_{py}-C_{im}$ and $C_{im}-N_{im}$ bond lengths in DIMPY complexes usually provide an indication of the extent of metal-to-ligand electron transfer,^{2,5,32} although sometimes disorder and/or (partial) ligand deprotonation make interpretation of the observed bond lengths difficult; for $LFeX$ complexes, they support the assignment as $L^-Fe^{II}X$.³³ For halide complexes, ligand reduction does not appear to affect the metal spin state, which remains high-spin Fe^{II} .⁵ Also, iron alkyl derivatives $LFeR_2$ and $LFeR$ have the same spin state and electronic structure as the analogous halides.^{28,32}

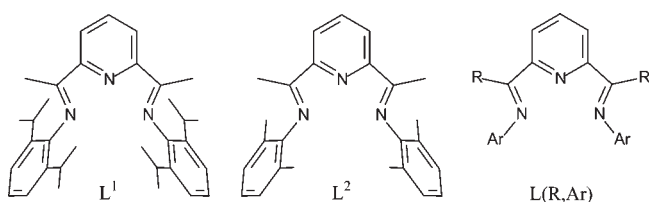
For cobalt, the situation is slightly different. While the dihalides are high-spin ($S = 3/2$),³⁴ the spin state of the monohalides $LCoX$ depends on the details of the ligand structure. With *aryl* groups at the nitrogen atom, the monohalides are diamagnetic^{35,36} ($S = 0$) and are best viewed as having a ligand radical anion ($S = 1/2$) antiferromagnetically coupled to a *low-spin* Co^{II} ($S = 1/2$) center.⁸ With *alkyl* groups at the nitrogen atom, the same electronic structure is observed at low temperature, but at higher temperatures, crossover to a paramagnetic state ($S = 1$) occurs, which was interpreted as having high-spin Co^{II} ($S = 3/2$) antiferromagnetically coupled to the ligand radical anion.³⁷ Dialkyl complexes $LCoR_2$ have not been observed so far and are probably unstable.^{38,39} The corresponding monoalkyl complexes $LCoR$ seem to be diamagnetic regardless of the ligand substitution pattern^{35–37} and are again best viewed as having a ligand radical anion antiferromagnetically coupled to low-spin Co^{II} . Though diamagnetic, these singlet-biradical-like complexes show some peculiar ¹H NMR chemical shifts (pyridine H4 signal around 10 ppm; imine methyl signals at 0 to -2 ppm). These unusual shifts were originally attributed to the thermal population of a low-lying triplet state,⁸ and the direct

Received: January 31, 2011

Published: April 26, 2011

Scheme 1. Some Common π -Acceptor Ligands

Scheme 2. Notation Used Here for DIMPY Ligands



observation of such a thermal population for *N*-alkylcobalt(I) halide complexes³⁷ supports this interpretation. However, the even more extreme shifts found for $\text{LFe}(\text{N}_2)_2$ complexes have been attributed to residual temperature-independent paramagnetism (TIP; singlet–triplet mixing caused by spin–orbit coupling^{32,40,41}) rather than thermally populated triplet states, and if that explanation is correct, a contribution from TIP for LCoR and LCoX complexes (in addition to, or instead of, a thermal triplet population) seems likely as well. More studies are probably needed to resolve the TIP versus thermal population issue.

Apart from the unexceptional LNiX_2 complexes,⁴² much less is known about the chemistry of nickel complexes of DIMPY ligands. One well-characterized monohalide (L^1NiCl) has been reported so far,⁴³ and bond lengths support a description with a low-spin Ni^{II} center and a ligand radical anion. We here report on the first monoalkyl complex, L^1NiMe , prepared via the somewhat unconventional route of treating $\text{LNi}(\text{N}_2)_2$ (vide infra) with trimethylaluminum (we will discuss the mechanism of this reaction later in this overview). The complex (Figure 1) shows the nickel atom in a standard square-planar environment. In view of the discussion above, this complex most likely contains low-spin Ni^{II} bound to a ligand radical anion; bond lengths in the X-ray structure are consistent with the transfer of 1–2 electrons from metal to ligand.

■ ELECTRONIC STRUCTURES OF DINITROGEN COMPLEXES

For both iron and cobalt, a number of dinitrogen complexes have been reported; in the present work, we add the new complex $\text{L}^1\text{Ni}(\text{N}_2)_2$ to the collection. Dinitrogen complexes are interesting by themselves but also as sources of reactive LM fragments, as will be discussed below. The group of Chirik has prepared mononuclear $\text{LFe}(\text{N}_2)_2$ complexes (bearing 2,6-*i*-Pr₂C₆H₃ groups at the nitrogen atom^{40,44}) as well as several binuclear $[\text{LFe}(\text{N}_2)]_2(\mu\text{-N}_2)$

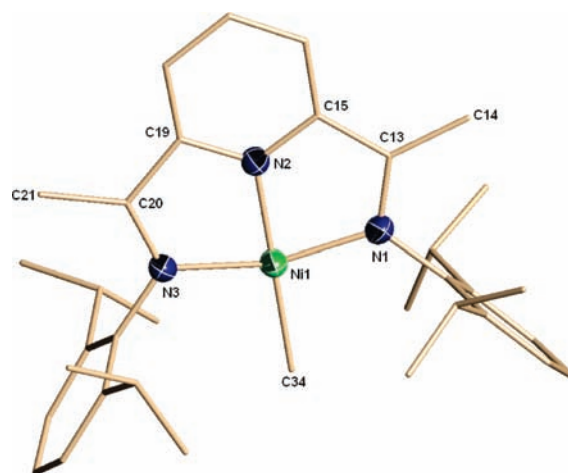


Figure 1. Partial thermal ellipsoid plot of L^1NiMe , drawn at the 50% probability level.

complexes (bearing less bulky 2,6-Et₂C₆H₃ and 2,6-Me₂C₆H₃ groups at the nitrogen atom).^{40,41} In all cases, the complexes are diamagnetic, containing intermediate-spin Fe^{II} ($S = 1$) antiferromagnetically coupled to a triplet ligand diradical dianion ($S = 1$). Interestingly, the anion $\text{LFe}(\text{N}_2)(\text{CH}_2\text{CMe}_3)^-$ was proposed to contain low-spin Fe^{II} ($S = 0$) and a closed-shell ($S = 0$) ligand dianion;⁴⁵ the reason for the apparently different electronic structures of the two types of complexes is not clear. In any case, the reduction from LFeX_2 to LFeX and then $\text{LFe}(\text{N}_2)_2$ seems to occur exclusively at the ligand, but the stronger ligand field of the reduced ligand induces a flip of one [in $\text{LFe}(\text{N}_2)_2$ ⁴¹] or two [in $\text{LFe}(\text{N}_2)(\text{CH}_2\text{CMe}_3)^-$ ⁴⁵] electrons at the metal. Several anionic dinitrogen complexes have also been prepared, and these still appear to contain Fe^{II} : apparently, a third electron can be accepted by the ligand, but calculations indicate that, upon the addition of a fourth electron, the metal would finally get reduced.⁴⁶

Again, the situation is markedly different for cobalt. The diamagnetic cationic complex $\text{LCo}(\text{N}_2)^+$, unlike neutral LCoX/LCoR , seems to contain true low-spin Co^{I} ($S = 0$) and a neutral, innocent DIMPY ligand. Interestingly, the unusual ¹H NMR shifts observed for the “non-innocent” LCoX/LCoR complexes (vide supra) are not found for the “innocent” $\text{LCo}(\text{N}_2)^+$ complex or for the analogous ethene complex.⁴⁷

One-electron reduction to neutral $\text{LCo}(\text{N}_2)$ occurs at the ligand, and a further one-electron reduction yields diamagnetic $\text{LCo}(\text{N}_2)^-$ still containing low-spin Co^{I} but now bound to a closed-shell ligand dianion.⁴⁸ Thus, compared to iron, cobalt seems to be more easily reduced to the univalent state. The different bonding interactions in LCoX ($\text{L}^0\text{Co}^{\text{II}}_{\text{LS}}$) and $\text{LCo}(\text{N}_2)^+$ ($\text{L}^0\text{Co}^{\text{I}}_{\text{LS}}$) reflect the weaker donating power of dinitrogen compared to halide or alkyl, resulting in a lowered stability of Co^{II} versus Co^{I} . At the same time, it is clear that metal-centered and ligand-centered reduction do not differ much in energy for the LCo^{II} fragment.

Only a handful of nickel–dinitrogen complexes have been reported to date.^{49–52} The new complex $\text{L}^1\text{Ni}(\text{N}_2)_2$ was prepared by stirring a yellowish-brown suspension of L^1NiBr_2 in tetrahydrofuran for 4 days at room temperature with 2 equiv of NaH. A bright burgundy solution was formed, which after workup gave the crystalline and diamagnetic dinitrogen complex; the X-ray structure (Figure 2) shows an approximately square-planar nickel metal center surrounded by the terdentate ligand and one

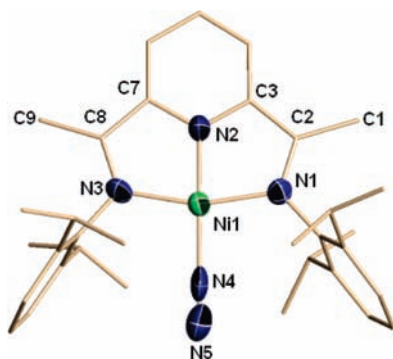


Figure 2. Partial thermal ellipsoid plot of $L^1Ni(N_2)$, drawn at the 50% probability level.

terminally bonded dinitrogen unit. The dinitrogen $N\equiv N$ bond distance ($N4-N5 = 0.92 \text{ \AA}$) is extremely short, indicative of the absence of any significant dinitrogen activation. The fact that the $N-N$ distance is even shorter than that in free dinitrogen is probably a crystallographic artifact due to nitrogen atom thermal motions or some minor disorder that could not be modeled. In agreement with the minimal extent of reduction of the $N\equiv N$ bond, the IR stretching was found at a high frequency (2156 cm^{-1}).

It is not immediately obvious how the bonding in $L^1Ni(N_2)$ should be interpreted. Possibilities are (a) Ni^0 and a neutral (innocent) ligand, (b) low-spin Ni^{II} and a closed-shell dianionic ligand,⁵³ or (c) the intermediate situation, Ni^I antiferromagnetically coupled to a ligand radical anion. All well-characterized $Ni(N_2)$ complexes reported to date contain Ni^0 , which would argue for option a. On the other hand, the dinitrogen appears to be very weakly bound in this complex. Also, Ni^0 prefers a tetrahedral environment; the approximately square-planar one found for our complex is more typical for Ni^{II} , which would support option b. Ni^I is not a very common oxidation state, and its geometric preferences are probably less pronounced. The $C_{py}-C_{im}$ and $C_{im}-N_{im}$ bond lengths in the X-ray structure are very similar to those found for L^1NiMe and would be consistent with a transfer of 1–2 electrons to the ligand, arguing in favor of option c. The complex is isoelectronic with $LCo(N_2)^-$, and for simplicity, we assume here an analogous electronic structure, i.e., low-spin Ni^{II} and a closed-shell ligand dianion. It should be noted here that none of the iron-, cobalt-, and nickel–dinitrogen complexes to date show evidence of strong activation of the dinitrogen ligand.

■ REACTIVITY OF DINITROGEN COMPLEXES

Regardless of whether the dinitrogen complexes contain a reduced metal or a reduced ligand (or both), one would expect them to be strong reductants, strong enough perhaps to break $C-X$ bonds. Indeed, Chirik et al. reported that the formally iron(0) complex $LFe(N_2)_2$ is able to break the activated $C-O$ bonds of esters and allyl ethers.⁵⁴ The mechanism proposed for this reaction involves a “classical” oxidative addition of $R-OR'$ to one iron center, followed by the loss of an R radical, which is then captured by a second iron(0) complex, yielding ultimately a mixture of $LFeOR'$ and $LFeR$. Supporting this mechanism is the isolation of $LFe(OAc)(\eta^1-C_2H_3)$, where apparently the loss of a vinyl radical does not occur. Alkyl halides RX also react with $LFe(N_2)_2$ to give mixtures of $LFeX$ and $LFeR$.³³

Table 1. C–C Coupling Reactions with L^2CoAr^a

entry	Ar	RX	products ^b
1	$C_6H_4-4-CF_3$	allylCl	allylAr (M), ArAr (m) ^c
2	C_6H_5	allylCl	allylAr (M), ArAr (m) ^c
3	$C_6H_4-4-OMe$	allylCl	allylAr (M), ArAr (m) ^c
4	C_6H_4-4-Cl	BzCl	BzAr (M), BzBz (M)
5	C_6H_5	<i>n</i> - $C_6H_{13}Br$	N.R.
6	$C_6H_4-4-CF_3$	BzBr	BzAr (m), BzBz (M), ArAr (tr)
7	C_6H_5	BzCl	BzAr (3.5), BzBz (1.0), ArAr (0.03)
8	$CH_2SiMe_3^d$	MeI	EtSiMe ₃
9	$C_6H_5^e$	PhI	N.R.
10	2- $C_5H_3N-6-Cl$	BzCl	N.R.
11	2- $C_5H_3N-6-Cl$	BzBr ^f	BzAr (m), BzBz (M) ^g

^a Mixture of L^2CoAr and L^2CoCl generated from $L^2Co(N_2)$ as described in ref 55, and then RX added (0.5 equiv relative to the original $ArCl$ used). ^b Detected by GC/MS. For entry 7, the amounts were calibrated against authentic samples. Other entries (not calibrated): M = major, m = minor, tr = trace product. ^c Some 1,5-hexadiene may have been formed but would not have been detected by GC/MS analysis. ^d Using separately prepared pure $L^2CoCH_2SiMe_3$ and 1.8 equiv of CH_3I ; product identified by NMR. ^e Using separately prepared pure L^2CoPh instead of the mixture with $LCoCl$. ^f Using 2.0 equiv of BzBr relative to $L^2Co(N_2)$. ^g The BzBz major product is derived mainly from the reaction of BzBr with $LCoCl$, which is faster than the reaction with $LCo-2-C_5H_3N-6-Cl$; BzCl does not react with $LCoCl$.

We recently investigated the reaction of $LCo(N_2)$ with both alkyl and aryl halides.⁵⁵ Aryl halides are, in general, more difficult to activate than alkyl halides, and chlorides are usually less reactive than bromides. Gratifyingly, we found that even aryl chlorides react with $LCo(N_2)$ to give a mixture of $LCoAr$ and $LCoCl$, though generally in a ratio smaller than 1:1. The choice of the DIMPY ligand proves to be crucial: with L^1 , the reaction produces only small amounts of L^1CoAr (about 15% relative to L^1CoCl for 4-trifluorochlorobenzene; for details, see the Supporting Information), whereas the less hindered ligand L^2 gives much better ratios (>0.7:1 for most aryl chlorides).⁵⁵ The mechanism proposed for this reaction, and supported by calculations, is direct halide abstraction from $ArCl$ by an LCo fragment, leading to $LCoCl$ and a free Ar radical, which then mostly finds its way to a second cobalt center. Interestingly, more reactive substrates (aryl bromides and iodides), though reacting more quickly, give poorer yields of $LCoAr$ products, possibly because of the higher free-radical concentration during the reaction.

We have now also investigated the potential of L^2CoAr complexes for C–C coupling reactions. A mixture of L^2CoAr and L^2CoCl was generated by treating $L^2CoCH_2SiMe_3$ first with H_2/N_2 and then with 0.5 equiv of $ArCl$ as described earlier,⁵⁵ and to this mixture was then added a second organic halide in excess (see the Supporting Information for details). Results are summarized in Table 1. L^2CoAr reacts only with activated alkyl halides like benzyl bromide, benzyl chloride, or allyl chloride, giving a mixture of products; e.g., for $L^2CoPh + BzCl$ (entry 7), $BzBz:BzPh:PhPh \approx 1:3.5:0.03$, consistent with a radical-type mechanism. As mentioned above, $L^2Co(N_2)$ is a strong enough reductant to abstract a halide from $ArCl$. In contrast, L^2CoAr is a much weaker reductant and can only abstract a halogen atom from activated halides like BzBr. Also, L^2CoAr complexes with electron-poor aryls should be poorer reductants and indeed require more highly activated halides to react: compare entries

7, 10, and 11. We propose that, after abstraction of bromide by L^2CoAr , the intermediate $L^2Co(Ar)(Br)$ quickly loses the aryl group as a radical, which mostly combines with the previously generated benzyl radical. This mechanism, based on the instability of $LCo(Ar)(Br)$, is consistent with the previously reported easy loss of an alkyl radical from $LCoR_2$.^{38,56} Alkyl–alkyl couplings are also possible, as illustrated by the formation of Me_3SiEt from $LCoCH_2SiMe_3$ and MeI (entry 8).

The reactivity and C–C coupling potential of $LNi(N_2)$ and $LNiR$ complexes are yet to be explored. However, (TERPY)NiR complexes are active in C–C coupling reactions, most likely involving a radical mechanism,^{57,58} so DIMPY complexes might well show similar reactivity.⁵⁹

LIGAND NON-INNOCENCE AND RADICAL CHEMISTRY

Ligand alkylation and the loss of alkyl groups is a recurring theme in the chemistry of metal–alkyl complexes of DIMPY ligands. Alkylation can even be reversible.^{23–25,27–29} We believe that much of this chemistry can be interpreted in terms of radical formation induced by the electronic non-innocence of the DIMPY ligand. In effect, the neutral DIMPY ligand, terdentate coordinated to the metal, is a strong oxidant, even capable of abstracting an electron from a metal–carbon bonding orbital, thus leading to easy loss of an organic radical. Where that radical then ends up depends on the details of the system like the size and stability of the alkyl, steric hindrance of the DIMPY ligand, nature of the central metal atom, and distribution of an unpaired electron density over the ligand. The binuclear oxidative addition of $ArCl$ to $L^2Co(N_2)$ can be explained in this way (Scheme 3); the C–C coupling reactions mentioned earlier can be rationalized in a similar manner (Scheme 4): $L^{\cdot}Co^{II}Ar$ first abstracts a halide from $BzBr$ to form $L^0Co^{II}(Ar)(Br)$, and then L^0 oxidizes the Co – Ar bond to give $L^{\cdot}Co^{II}Br$ and Ar^{\cdot} . Thus, C–C coupling would be another illustration of the “ennobling” character of redox-active ligands in combination with first-row transition metals.⁶⁰

This idea of ligand-induced radical formation can also explain why alkylation at various positions of the ligand happens with comparable ease for main-group metals (Li, Mg, Zn, and Al) and transition metals (V, Cr, and Fe).² Preliminary calculations on simple aluminum model systems (see Table 2) support the extreme stabilization of low oxidation states by the π -acceptor ligands in Scheme 1 and, hence, facilitation of the loss of an alkyl

radical. This stabilization is nearly enough to make ejection of even the highly reactive methyl radical thermoneutral and explains the easy release of R radicals from $LCoR_2$ mentioned earlier.

Returning now to the mechanism of L^1NiMe formation from $L^1Ni(N_2)$ and $AlMe_3$, this can be rationalized by similar radical chemistry. The first step would likely be expulsion of nickel from its complex by aluminum. This would initially form L^1AlMe_3 , which would eject a methyl radical, giving L^1AlMe_2 (such a species was isolated and fully characterized from a similar reaction of the iron congener¹⁰). The released methyl radical would then find its way to a second $L^1Ni(N_2)$ molecule and bind to the nickel atom (Scheme 5), similar to the formation of L^2CoAr from $L^2Co(N_2)$ and Ar in Scheme 3.

Scheme 4. C–C Coupling Using $LCoAr$ ⁶¹

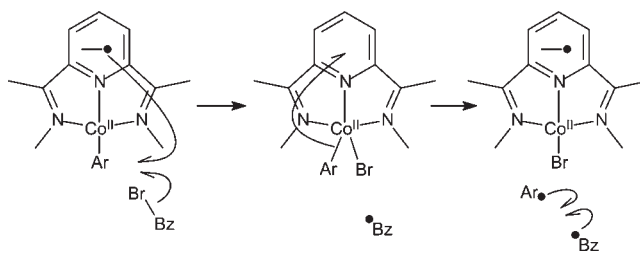
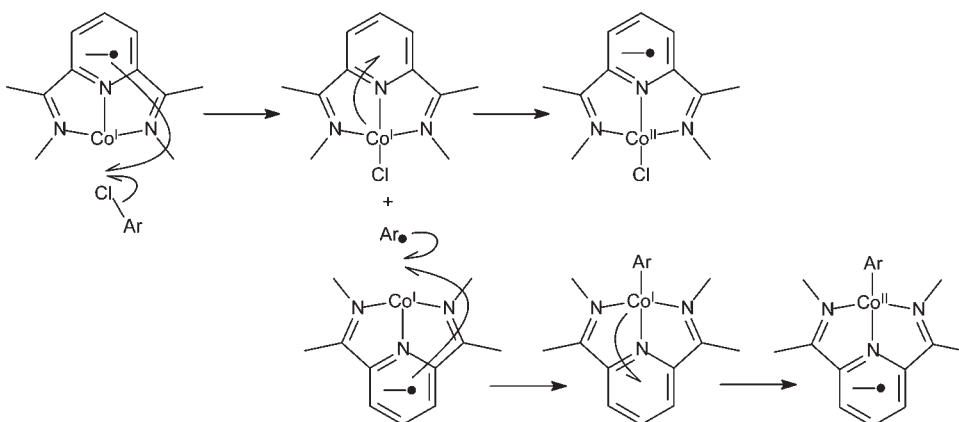


Table 2. Reaction Energies (kcal/mol)^a for the Loss of a Methyl Radical from $AlMe_3$ Complexes

ligand ^b	$LAlMe_3 \rightarrow LAlMe_2 + Me^{\cdot}$			
	Me at N		2,6-Me ₂ C ₆ H ₃ at N	
	E_{rxn}	E_{act}	E_{rxn}	E_{act}
(none)	81.0			
TMEDA	82.7			
DIM	8.3	13.4	7.0	18.9
IMPY	16.5	22.2	15.1	21.3
BIPY	19.7	25.0		
DIMPY	6.5	21.8	15.3	32.1 ^c

^a Electronic energies only, ub3-lyp/SV(P), not corrected for zero-point energies, thermal effects, or solvent effects. ^b For ligand abbreviations, see Scheme 1. ^c For κ^3 DIMPY coordination; a path involving a κ^2 -coordinated ligand (like IMPY) is probably more reasonable.

Scheme 3. Radical-Type Oxidative Addition at LCo Fragments⁶¹



UNUSUAL COORDINATION MODES

The DIMPY ligand is usually assumed to coordinate in a terdentate fashion. However, we here report an example from nickel chemistry that illustrates a surprisingly different coordination mode. If the synthesis of $L^1Ni(N_2)$ is attempted by combining in situ $NiBr_2(DME)$, L^1 , and 3 equiv of NaH , a different and paramagnetic complex was obtained. The same new complex is obtained if previously isolated $L^1Ni(N_2)$ is treated with ethylene or toluene to attempt replacement of the labile dinitrogen ligand (Scheme 6).

A single-crystal X-ray diffraction study revealed the complex to contain a dimerized ligand, here indicated as L^1-L^1 , wrapped around two nickel atoms, which have no other ligands bound to them (Figure 3). It is a symmetry-generated dimer consisting of two ligand systems and two nickel centers. The two ligands are linked by a C–C bond between the two former imine methyl groups, which in the process have lost one hydrogen each. Each ligand half-chelates one nickel atom with an iminepyridine fragment [$Ni1-N1 = 1.961(3) \text{ \AA}$; $Ni1-N2 = 1.909(3) \text{ \AA}$] and uses its second imine function (at which it has dimerized) to η^2 -coordinate to the other nickel atom [$Ni1-N3 = 1.902(3) \text{ \AA}$; $Ni1-C21 = 1.916(4) \text{ \AA}$]. This second imine group is visibly elongated [$N3-C21 = 1.398(5) \text{ \AA}$] relative to the first one [$N1-C13 = 1.291(5) \text{ \AA}$], indicating extensive back-donation from the formally Ni^0 metal center.⁶² The remaining imine methyl group appears to be intact, with a C–Me distance as expected for a single bond [$C13-C14 = 1.513(6) \text{ \AA}$]. The tetracoordinate geometry around each nickel center is severely distorted, with angles of $N1-Ni1-N2 = 83.24(14)^\circ$, $N2-Ni1-N3 = 148.74(14)^\circ$, $N1-Ni1-N3 = 124.55(14)^\circ$, and $N2-Ni1-C21 = 106.30(15)^\circ$.

The ligand dimerization has precedents in Mn^6 and Co^63 chemistry and arises from deprotonation of one of the two imine methyl groups and coupling of the resulting CH_2 unit with an identical one from a second unit. This transformation clearly arises from one-electron transfer to the imine functionality. The release of a hydrogen atom, possibly as a radical hydrogen transfer to some acceptor, results in the formation of a CH_2 radical of sufficiently long lifetime to enable dimerization. The manner in which the dimerized ligand of $(L^1-L^1)Ni_2$ is bound to both nickel atoms is unprecedented; the manganese and cobalt examples mentioned above show the much less surprising $\kappa^3:\kappa^3$ coordination mode.

Sometimes, unusual coordination modes of ligands like DIM-PY might be obtained because a metal salt and L are combined

Scheme 6. Different Routes toward $(L^1-L^1)Ni_2$

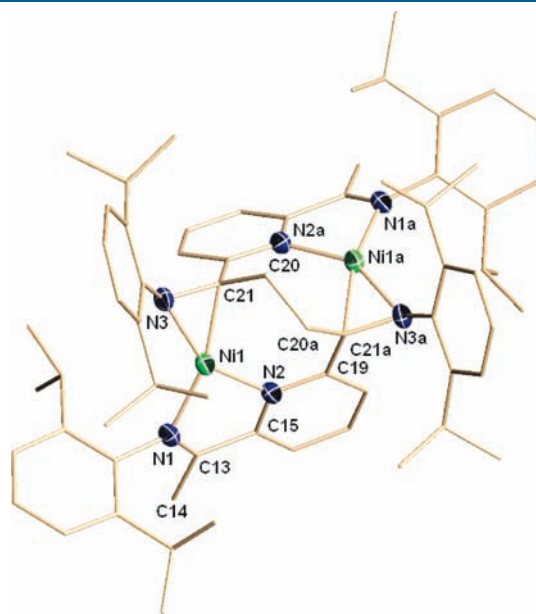
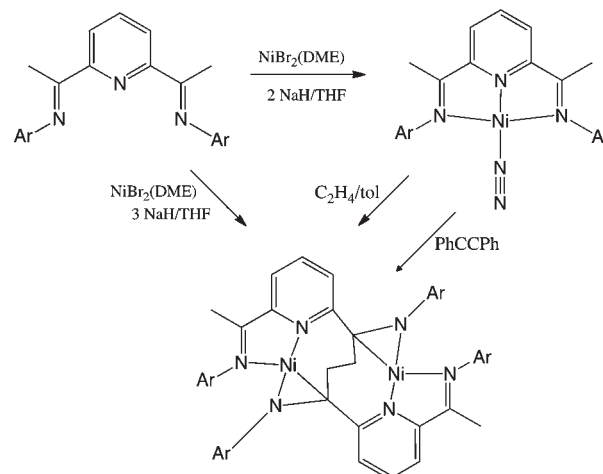


Figure 3. Partial thermal ellipsoid plot of $(L^1-L^1)Ni_2$, drawn at the 50% probability level. Hydrogen atoms are omitted for clarity.

Scheme 5. Possible Mechanism for the Formation of L^1NiMe from $L^1Ni(N_2)$ and $AlMe_3$ ⁶¹

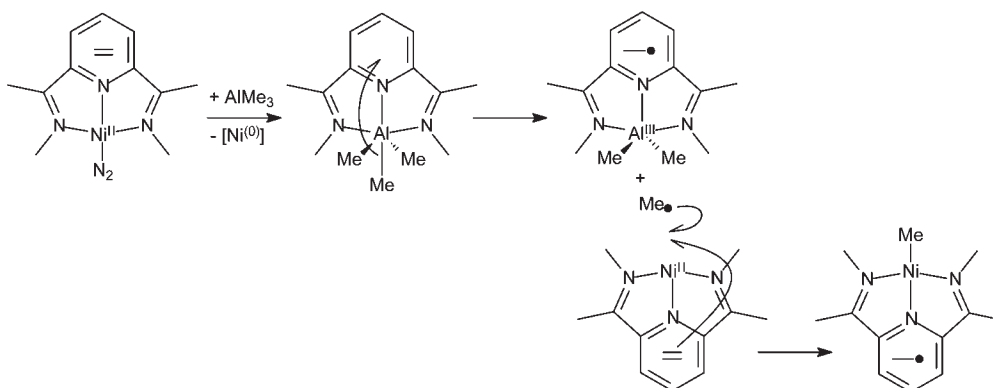


Table 3. Details of X-ray Structure Determinations

	(L ¹ -L ¹)		
	L ¹ Ni(N ₂)	L ¹ NiMe	Ni ₂ ·4 THF·Et ₂ O
formula	C ₃₃ H ₄₃ N ₅ Ni	C ₃₄ H ₄₆ N ₃ Ni	C ₈₆ H ₁₂₆ N ₆ Ni ₂ O ₅
M _w	568.43	555.45	1441.35
T (K)	200(2)	202(2)	202(2)
wavelength (Å)	0.710 73	0.710 73	0.710 73
cryst syst	orthorhombic	monoclinic	monoclinic
space group	P2 ₁ 2 ₁	P2 ₁ /c	C2/c
a (Å)	8.5334(11)	15.268(8)	26.340(3)
b (Å)	17.997(2)	14.920(8)	13.5083(14)
c (Å)	20.322(3)	14.715(8)	24.279(3)
α (deg)	90	90	90
β (deg)	90	112.557(7)	109.447(2)
γ (deg)	90	90	90
V (Å ³)	3120.9(7)	3096(3)	8145.6(15)
Z	4	4	4
D _{calcd} (Mg/m ³)	1.210	1.192	1.175
abs coeff (mm ⁻¹)	0.650	0.652	0.515
F(000)	1216	1196	3120
R1, R _w 2	0.0553, 0.1243	0.0561, 0.1328	0.0635, 0.1539
GOF	0.991	1.040	1.051

in situ and maybe never arrive at the standard terdentate coordination mode; that might apply to the synthesis of (L¹-L¹)Ni₂ from L¹, NiBr₂(DME), and NaH in Scheme 6. However, in the ethylene and toluene reactions also reported here, the ligand starts out terdentate and opens up at some point, showing that terdentate coordination should not be identified with rigid, fixed, and unbreakable coordination. Flexible coordination modes are obviously important during the initial complexation of the ligand to a metal. In addition, the temporary (or permanent) opening of the terdentate chelation⁶⁴ may well be relevant in many reactions of DIMPY complexes.

CONCLUSIONS AND OUTLOOK

The DIMPY ligand is capable of promoting an unprecedented diversity of chemical reactions, both at the metal and at the ligand itself. While the original application of the ligand in polymerization catalysis^{34,65} is probably not directly connected to its non-innocent character,⁶⁶ many other aspects of its chemistry are likely to be intimately connected to metal-to-ligand electron transfer.⁶⁷ In particular, we propose that ligand non-innocence and alkyl/aryl radical chemistry are two sides of the same coin. One of the more exciting aspects of the C-C coupling reaction described here is that, although it superficially resembles the one catalyzed by noble metals, the mechanism is clearly different, which may well lead to different selectivities, functional-group tolerance, and areas of application. The versatility of coordination modes, not available to other “staple” ligands like cyclopentadienyls, might also be relevant in reactions of DIMPY complexes. It seems obvious that this ligand has more surprises in store.

EXPERIMENTAL SECTION

General Considerations. All experiments were performed under an argon atmosphere using standard Schlenk techniques or in a nitrogen-filled drybox. Pentane, toluene, diethyl ether, tetrahydrofuran (THF),

benzene, THF-*d*₈, and benzene-*d*₆ were distilled from sodium/benzophenone. 4-CF₃C₆H₄Cl was purchased from Aldrich, degassed, and dried over 4 Å molecular sieves before use. Sodium hydride was purchased from Aldrich and washed with hexane under nitrogen to remove the oil. NiBr₂(DME) was obtained from Strem Chemicals. The ligand L¹,³⁴ complex L¹Co(N₂),^{48,55} mixtures of L²CoAr and L²CoCl,⁵⁵ and pure L²CoAr⁵⁵ were prepared according to published procedures.

IR spectra were recorded on an ABB Bomen Fourier transform infrared (FTIR) instrument from Nujol mulls prepared in a drybox except in the case of air-stable compounds. Samples for magnetic susceptibility were preweighed inside a drybox equipped with an analytical balance and measured on a Johnson Matthey 2400 CHN analyzer. Magnetic moments were calculated following standard methods, and corrections for the diamagnetisms were applied to the data. Data for X-ray crystal structure determination were obtained with a Bruker diffractometer equipped with a SMART 1K CCD area detector.

¹H NMR, ¹³C{H} NMR, ²⁹Si{H} NMR, and ¹⁹F NMR spectra were recorded on Bruker Avance 300 and 500 MHz spectrometers. All ¹H and ¹³C NMR shifts (δ, ppm) were referenced to the solvent (for benzene-*d*₆, ¹H NMR, C₆D₅H δ 7.16 ppm, and ¹³C NMR, C₆D₆ δ 128.0 ppm; for CDCl₃, ¹H NMR, CHCl₃ δ 7.26 ppm, and ¹³C NMR, CDCl₃ δ 77.0 ppm). ¹⁹F{H} NMR spectra were referenced to internal benzotrifluoride in benzene-*d*₆ (δ -62.4 ppm). Data were collected at room temperature unless otherwise noted. Gas chromatography/mass spectrometry (GC/MS) instrument: Varian 3800 gas chromatograph with a 30 m VF-5 ms column coupled to a Varian 320 mass spectrometer operated in single quadrupole mode.

Reaction between L¹Co(N₂) and 4-CF₃C₆H₄Cl. In a dinitrogen-filled drybox, L¹Co(N₂) (11.8 mg, 20 μmol) was weighed and dissolved in about 0.4 mL of dry benzene-*d*₆, and 4-CF₃C₆H₄Cl (2.45 μL, 19.6 μmol) was added. The mixture turned gray-blue. The immediately recorded ¹H NMR spectrum showed that the reaction was not complete [L¹Co(N₂) was still visible] and three diamagnetic cobalt(I) complexes could be clearly observed: L¹CoH:L¹CoAr:L¹CoCl = 0.11:0.14:1.00. After 4 h, the ¹H NMR spectrum showed that there was no L¹Co(N₂) left and the reaction was complete, with product ratio L¹CoH:L¹CoAr:L¹CoCl = 0.045:0.14:1.00. Assignments for L¹CoH and L¹CoCl are based on literature values⁴⁷ and those for L¹CoAr on analogy with previously reported L²CoAr.⁵⁵

Tentative, partial assignments for L¹CoAr. ¹H NMR (25 °C, benzene-*d*₆, 300 MHz): δ 10.27 (1H, t, J = 7.6 Hz, Py H4), 5.14 (2H, d, J = 7.1 Hz, CoAr H2), -0.65 (6H, s, CH₃C=N). ¹⁹F NMR (25 °C, benzene-*d*₆, 282 MHz): δ -61.2.

Reaction of L²CoCH₂SiMe₃ with CH₃I. In a drybox, L²CoCH₂SiMe₃ (37.5 mg, 72 μmol) was dissolved in benzene-*d*₆, followed by injection of 8 μL of CH₃I (130 μmol, 1.8 equiv). The mixture immediately turned pink. ¹H NMR showed only broad peaks. After 30 min, a lot of solid had precipitated. In a drybox, this sample was filtered over glass wool, and the filtrate was analyzed by ¹H NMR, but the peaks were still too broad for useful interpretation. Around 0.5 mL of air was injected into the NMR tube to quench any paramagnetic cobalt complexes, and after shaking, the sample was quickly filtered over glass wool in air. ¹H NMR obtained in this way (Figure S1 in the Supporting Information) had reasonable line widths and showed a new quartet at δ 0.45 ppm (J = 8.0 Hz). GC/MS analysis of this NMR sample clearly showed that EtSiMe₃ was the main compound, and ¹H-²⁹Si HMBC (Figure S2 in the Supporting Information) also confirmed that the ethyl and methyl groups were attached to the same silicon atom.

C-C Coupling Reactions. A mixture of LCoAr and LCoX was generated as described previously,⁵⁵ by treating 27 μmol of L²CoCH₂SiMe₃ in 0.4 mL of benzene-*d*₆ with H₂ in the presence of N₂ and then adding 27 μmol of ArX. To this mixture was added with a syringe 0.5 equiv (relative to ArX) of the alkyl halide. For benzyl bromide and methyl iodide, the reaction is instantaneous; for benzyl chloride and allyl chloride,

it takes hours to complete. The mixture turned to green and deposited black solids. After the sample had turned gray, 0.5 mL of water was added. The organic layer was filtered over glass wool and analyzed by GC/MS. This procedure was followed for all entries except entry 8 in Table 1.

$L^1Ni(\eta^1-N_2)$. Solid $NiBr_2(DME)$ (0.154 g, 0.5 mmol) and ligand L^1 (0.241 g, 0.5 mmol) were mixed together in THF (15 mL) and allowed to stir for 2 days at room temperature, resulting in a brown suspension. Solid NaH (0.025 g, 1.05 mmol) was added to the suspension, and stirring was continued at room temperature for 4 days. During this time, the suspension became dark purple. The suspension was then dried under vacuum, and the residue was suspended in hexane and centrifuged to remove undissolved materials and excess NaH. The resulting dark-purple supernatant was concentrated to 5 mL and left undisturbed at $-35\text{ }^\circ\text{C}$ for 4 days. Dark-purple diamagnetic crystals of X-ray quality were formed (0.200 g, 0.35 mmol, 70%).

IR (cm^{-1} , Nujol mull): 2922, 2854 (Nujol), 2156 (N_2), 1580 (w, s), 1457 (w), 1377 (s), 1283 (w, s), 125 (m), 1120, 1053, 960, 807, 760, 665. ^1H NMR (C_6D_6 , 300 MHz, $25\text{ }^\circ\text{C}$): δ 7.50 (2H, d, $J = 7.5\text{ Hz}$, Py H3), 7.23 (6H, s, Ar), 6.90 (1H, t, $J = 7.5\text{ Hz}$, Py H4), 3.41 (4H, sept, $CHMe_2$), 1.57 (6H, s, $MeC=N$), 1.49 (12H, d, $J = 6.9\text{ Hz}$, $CHMe_2$), 1.13 (12H, d, $J = 6.9\text{ Hz}$, $CHMe_2$). ^{13}C NMR (C_6D_6): δ 149.6, 146.9, 140.2, 139.5, 126.3, 124.4, 123.2, 111.4, 27.9 ($CHMe_2$), 24.5 ($MeC=N$), 24.0 ($CHMe_2$), 16.7 ($CHMe_2$).

L^1NiMe . Dark-purple crystals of $L^1Ni(N_2)$ (0.100 g, 0.175 mmol) were dissolved in toluene (5 mL). Me_3Al (0.0126 g, 0.175 mmol) was added to the stirred solution, and stirring was continued at room temperature for another 30 min. The solution was then layered with an equal volume of hexane and left undisturbed at $-35\text{ }^\circ\text{C}$ for 7 days, yielding dark-brown, X-ray-quality, and paramagnetic crystals (0.06 g, 0.108 mmol, 62%). IR (Nujol mull, cm^{-1}): 2955, 2924.7, 2854.1 (Nujol), 1588 (w), 1457.3 (w), 1377.4 (s), 1321.2 (s), 1236.6, 1177.5 (w), 1078.7 (w), 935.75 (w), 862.08 (w, s), 789.86, 721.45, 698.6, 665.58 (s).

$(L^1-L^1)Ni_2$ Method A. Solid $NiBr_2(DME)$ (0.154 g, 0.5 mmol) and ligand L^1 (0.241 g, 0.5 mmol) were mixed together in THF (15 mL) and allowed to stir for 2 days at room temperature, affording a brown suspension. Solid NaH (0.039 g, 1.65 mmol) was added to the stirred suspension, and stirring was continued for 4 days. The resulting dark-purple suspension was dried under vacuum, and the residue was suspended in hexane and centrifuged to remove undissolved materials and excess of NaH. The dark-purple solution was concentrated to 5 mL and left undisturbed at $-35\text{ }^\circ\text{C}$ for 4 days, during which dark-brown X-ray-quality crystals of $(L^1-L^1)Ni_2$ were formed (0.220 g, 0.152 mmol, 30%).

IR (Nujol mull, cm^{-1}): 2956.5, 2924.1, 2854.2, 1644.3 (s), 1576.4 (s), 1461.6 (w), 1377.6 (s), 1366.6, 1325.8, 1325.8, 1254.8, 1192.7, 1124.3, 1105.3, 1055.9, 991.3 (w), 828.38, 768.22, 665.48 (s). $\mu_{\text{eff}} = 1.38\mu_{\text{BM}}$.

$(L^1-L^1)Ni_2$ Method B. Dark-purple crystals of $L^1Ni(N_2)$ (0.100 g, 0.175 mmol) were dissolved in toluene (10 mL). Ethylene gas (1 atm) was passed through the stirred solution, and stirring was continued at room temperature for 24 h, during which the solution became darker. The solution was then dried under vacuum, dissolved in hexane, and centrifuged to remove a small amount of undissolved solid. The dark supernatant was concentrated to 5 mL and left undisturbed at $-35\text{ }^\circ\text{C}$ for a few days, affording dark-brown crystals of $(L^1-L^1)Ni_2$ (0.061 g, 0.042 mmol, 24%).

$(L^1-L^1)Ni_2$ Method C. Dark-purple crystals of $L^1Ni(N_2)$ (0.100 g, 0.175 mmol) were dissolved in toluene (10 mL). Solid diphenylacetylene (0.3115 g, 0.175 mmol) was added to the stirred solution, and stirring was continued at room temperature for 24 h. The solution became darker and was dried under vacuum. The residue was dissolved in hexane, and the suspension was centrifuged to remove a small amount of undissolved residue. The dark supernatant was concentrated to 5 mL and left undisturbed at $-35\text{ }^\circ\text{C}$ for a few days to afford dark-brown crystals of $(L^1-L^1)Ni_2$ (0.079 g, 0.054 mmol, 31%).

Crystal Structure Determinations. Single crystals of complexes $L^1Ni(N_2)$, L^1NiMe , and $(L^1-L^1)Ni_2$ suitable for X-ray diffraction were selected under an inert atmosphere and mounted on a glass fiber. Unit cell measurements and intensity data collections were performed on a Bruker-AXS SMART 1K CCD diffractometer using graphite-monochromatized Mo $K\alpha$ radiation ($\lambda = 0.71073\text{ \AA}$). The data reduction included a correction for Lorentz and polarization effects, with an applied multiscan absorption correction (SADABS⁶⁸). The crystal structures were solved and refined using the *SHELXTL* program suite.⁶⁹ Direct methods yielded all non-hydrogen atoms, which were refined with anisotropic thermal parameters. All hydrogen atom positions were calculated geometrically and were riding on their respective atoms. The dinuclear complex $(L^1-L^1)Ni_2$ crystallized with disordered molecules of both THF and diethyl ether in the unit cell. The crystal data and refinement parameters for the complexes are listed in Table 3. Interatomic distances and angles are given in the Supporting Information for this paper; for further information, see the respective CIF files.

Computational Methods. All geometries were optimized with *Turbomole*^{70,71} using the SV(P) basis set,⁷² the b3-lyp functional,^{73–76} and the unrestricted density functional theory formalism in combination with an external optimizer (PQS OPTIMIZE).^{77,78} Transition states for methyl dissociation were calculated using a broken-symmetry $S_z = 0$ solution. Vibrational analyses were carried out to confirm the nature of all stationary points.

■ ASSOCIATED CONTENT

S Supporting Information. ^1H NMR and $^1\text{H}-^{29}\text{Si}$ HMBC spectra for the reaction product from $L^2CoCH_2SiMe_3$ and MeI, X-ray structure determinations, and crystallographic data in CIF format for the X-ray structures mentioned in the text. This material is available free of charge via the Internet at <http://pubs.acs.org>.

■ AUTHOR INFORMATION

Corresponding Author

*E-mail: Peter_Budzelaar@umanitoba.ca.

■ ACKNOWLEDGMENT

Financial support from the NSERC, CFI, MRIF, University of Manitoba, and University of Ottawa is gratefully acknowledged.

■ REFERENCES

- (1) General review of DIMPY and related ligands: Gibson, V. C.; Redshaw, C.; Solan, G. *Chem. Rev.* **2007**, *107*, 1745.
- (2) Review focusing on ligand non-innocence: Knijnenburg, Q.; Gambarotta, S.; Budzelaar, P. H. M. *Dalton Trans.* **2006**, 5442.
- (3) Wissing, E.; Van der Linden, S.; Rijnberg, E.; Boersma, J.; Smeets, W. J. J.; Spek, A. L.; Van Koten, G. *Organometallics* **1994**, *13*, 2602.
- (4) De Bruin, B.; Bill, E.; Bothe, E.; Weyhermüller, T.; Wieghardt, K. *Inorg. Chem.* **2000**, *39*, 2936.
- (5) Budzelaar, P. H. M.; De Bruin, B.; Gal, A. W.; Wieghardt, K.; Lenthe, J. H. *Inorg. Chem.* **2001**, *40*, 4649.
- (6) Reardon, D.; Aharonian, G.; Gambarotta, S.; Yap, G. P. A. *Organometallics* **2002**, *21*, 786.
- (7) Sugiyama, H.; Aharonian, G.; Gambarotta, S.; Yap, G. P. A.; Budzelaar, P. H. M. *J. Am. Chem. Soc.* **2002**, *124*, 12268.
- (8) Knijnenburg, Q.; Hettterscheid, D. G. H.; Kooistra, T. M.; Budzelaar, P. H. M. *Eur. J. Inorg. Chem.* **2004**, 1204.
- (9) Sugiyama, H.; Korobkov, I.; Gambarotta, S.; Möller, A.; Budzelaar, P. H. M. *Inorg. Chem.* **2004**, *43*, 5771.

- (10) Scott, J.; Gambarotta, S.; Korobkov, I.; Knijnenburg, Q.; De Bruin, B.; Budzelaar, P. H. M. *J. Am. Chem. Soc.* **2005**, *127*, 17204.
- (11) Bailey, P. J.; Dick, C. M.; Fabre, S.; Parsons, S.; Yellowlees, L. J. *Dalton Trans.* **2006**, 1602.
- (12) Van Koten, G.; Jastrzebski, T. B. H.; Vrieze, K. *J. Organomet. Chem.* **1983**, *250*, 49.
- (13) Kaupp, M.; Stoll, H.; Preuss, H.; Kaim, W.; Stahl, T.; Van Koten, G.; Wissing, E.; Smeets, W. J. J.; Spek, A. L. *J. Am. Chem. Soc.* **1991**, *113*, 5606.
- (14) Wissing, E.; Van Gorp, K.; Boersma, J.; Van Koten, G. *Inorg. Chim. Acta* **1994**, *220*, 55.
- (15) Wissing, E.; Rijnberg, E.; Van der Schaaf, A.; Van Gorp, K.; Boersma, J.; Van Koten, G. *Organometallics* **1994**, *13*, 2609.
- (16) Wissing, E.; Kaupp, M.; Boersma, J.; Spek, A. L.; Van Koten, G. *Organometallics* **1994**, *13*, 2349.
- (17) Gibson, V. C.; Redshaw, C.; White, A. J. P.; Williams, D. J. *J. Organomet. Chem.* **1998**, *550*, 453.
- (18) Riollet, V.; Copéret, C.; Basset, J. M.; Rousset, L.; Bouchu, D.; Grosvalet, L.; Perrin, M. *Angew. Chem., Int. Ed.* **2002**, *41*, 3025.
- (19) Fedushkin, I. L.; Tishkina, A. N.; Fukin, G. K.; Hummert, M.; Schumann, H. *Eur. J. Inorg. Chem.* **2008**, 483.
- (20) Spek, A. L.; Jastrzebski, T. B. H.; Van Koten, G. *Acta Crystallogr., Sect. C* **1987**, *43*, 2006.
- (21) Nienkemper, K.; Kehr, G.; Kehr, S.; Fröhlich, R.; Erke, G. *J. Organomet. Chem.* **2008**, *693*, 1572.
- (22) Bruce, M.; Gibson, V. C.; Redshaw, C.; Solan, G. A.; White, A. J. P.; Williams, D. J. *Chem. Commun.* **1998**, 2523.
- (23) Reardon, D.; Conan, F.; Gambarotta, S.; Yap, G. P. A.; Wang, Q. *J. Am. Chem. Soc.* **1999**, *121*, 9318.
- (24) Clentsmith, G. K. B.; Gibson, V. C.; Hitchcock, P. B.; Kimberley, B. S.; Rees, C. W. *Chem. Commun.* **2002**, 1498.
- (25) Khorobkov, I.; Gambarotta, S.; Yap, G. P. A. *Organometallics* **2002**, *21*, 3088.
- (26) Cameron, T. M.; Gordon, J. C.; Michalczyk, R.; Scott, B. L. *Chem. Commun.* **2003**, 2282.
- (27) Blackmore, I. J.; Gibson, V. C.; Hitchcock, P. B.; Rees, C. W.; Williams, D. J.; White, A. J. P. *J. Am. Chem. Soc.* **2005**, *127*, 6012.
- (28) Scott, J.; Gambarotta, S.; Korobkov, I.; Budzelaar, P. H. M. *J. Am. Chem. Soc.* **2005**, *127*, 13019.
- (29) Knijnenburg, Q.; Smits, J. M. M.; Budzelaar, P. H. M. *Organometallics* **2006**, *25*, 1036.
- (30) The involvement of radicals in the alkylation of DIM and IMPY ligands is well-established. See refs 3, 11–13, 15, and 16.
- (31) Radicals associated with the N-alkylation of DIMPY ligands have been observed. See ref 27.
- (32) Bart, S. C.; Chłopek, K.; Bill, E.; Bouwkamp, M. W.; Lobkovsky, E.; Neese, F.; Wieghardt, K.; Chirik, P. J. *J. Am. Chem. Soc.* **2006**, *128*, 13901.
- (33) Trovitch, R. J.; Lobkovsky, E.; Chirik, P. J. *J. Am. Chem. Soc.* **2008**, *130*, 11631.
- (34) Small, B. L.; Brookhart, M.; Bennett, A. M. A. *J. Am. Chem. Soc.* **1998**, *120*, 4049.
- (35) Gibson, V. C.; Humphries, M. J.; Tellmann, K. P.; Wass, D. F.; White, A. J. P.; Williams, D. J. *Chem. Commun.* **2001**, 2252.
- (36) Kooistra, T. M.; Knijnenburg, Q.; Smits, J. M. M.; Horton, A. D.; Budzelaar, P. H. M.; Gal, A. W. *Angew. Chem., Int. Ed.* **2001**, *40*, 4719.
- (37) Bowman, A. C.; Milsman, C.; Bill, E.; Lobkovsky, E.; Weyhermüller, T.; Wieghardt, K.; Chirik, P. J. *Inorg. Chem.* **2010**, *49*, 6110.
- (38) Zhu, D.; Janssen, F. F. B. J.; Budzelaar, P. H. M. *Organometallics* **2010**, *29*, 1897.
- (39) Treatment of $(\text{Py})_2\text{Co}(\text{CH}_2\text{SiMe}_3)_2$ with L^2 cleanly produces $\text{L}^2\text{CoCH}_2\text{SiMe}_3$ without any detectable intermediates. However, the same reaction with a PyBOX ligand initially forms paramagnetic $(\text{PyBOX})\text{Co}(\text{CH}_2\text{SiMe}_3)_2$, detected by $^1\text{H NMR}$.³⁸
- (40) Bart, S. C.; Lobkovsky, E.; Chirik, P. J. *J. Am. Chem. Soc.* **2004**, *126*, 13794.
- (41) Russell, S. K.; Darmon, J. M.; Lobkovsky, E.; Chirik, P. J. *Inorg. Chem.* **2010**, *49*, 2782.
- (42) Su, B.; Feng, G. *Polym. Int.* **2010**, *59*, 1058 and reference cited therein..
- (43) Manuel, T. D.; Rohde, J. U. *J. Am. Chem. Soc.* **2009**, *131*, 15582.
- (44) Archer, A. M.; Bouwkamp, M. W.; Cortez, M. P.; Lobkovsky, E.; Chirik, P. J. *Organometallics* **2006**, *25*, 4269.
- (45) Tondreau, A. M.; Milsman, C.; Patric, A. D.; Hoyt, H. M.; Lobkovsky, E.; Wieghardt, K.; Chirik, P. J. *J. Am. Chem. Soc.* **2010**, *132*, 15046.
- (46) Scott, J.; Vidyaratne, I.; Korobkov, I.; Gambarotta, S.; Budzelaar, P. H. M. *Inorg. Chem.* **2008**, *47*, 896.
- (47) Humphries, M. J.; Tellmann, K. P.; Gibson, V. C.; White, A. J. P.; Williams, D. J. *Organometallics* **2005**, *24*, 2039.
- (48) Bowman, A. C.; Milsman, C.; Atienza, C. C. H.; Lobkovsky, E.; Wieghardt, K.; Chirik, P. J. *J. Am. Chem. Soc.* **2010**, *132*, 1676.
- (49) Kruger, C.; Tsay, Y. H. *Angew. Chem.* **1973**, *85*, 1051.
- (50) Jolly, P. W.; Jonas, K.; Kruger, C.; Tsay, Y. H. *J. Organomet. Chem.* **1971**, *33*, 109.
- (51) Waterman, R.; Hillhouse, G. L. *Can. J. Chem.* **2005**, *83*, 328.
- (52) Pfirrmann, S.; Limberg, C.; Herwig, C.; Stosser, R.; Ziemer, B. *Angew. Chem., Int. Ed.* **2009**, *48*, 3357.
- (53) One could also think of high-spin Ni^{II} antiferromagnetically coupled to a triplet ligand dianion. However, for square-planar high-spin Ni^{II} , there would be one electron in the $d_{x^2-y^2}$ orbital that has the wrong symmetry to couple with a ligand π^* orbital. Therefore, we believe we can safely rule out this variation.
- (54) Trovitch, R. J.; Lobkovsky, E.; Bouwkamp, M. W.; Chirik, P. J. *Organometallics* **2008**, *27*, 6264.
- (55) Zhu, D.; Budzelaar, P. H. M. *Organometallics* **2010**, *29*, 5759.
- (56) Like in the previously studied reaction of $\text{LCo}(\text{N}_2)$ with organic halides,⁵⁵ we cannot exclude the fact that the actual mechanism of oxidative addition is substrate-dependent. In the absence of experimental evidence pointing either way, we here assume for simplicity a single common mechanism.
- (57) Anderson, T. J.; Jones, G. D.; Vivic, D. A. *J. Am. Chem. Soc.* **2004**, *126*, 8100.
- (58) Jones, G. D.; Martin, J. L.; McFarland, C.; Allen, O. R.; Hall, R. E.; Haley, A. D.; Brandon, R. J.; Konovalova, T.; Desrochers, P. J.; Pulay, P.; Vivic, D. A. *J. Am. Chem. Soc.* **2006**, *128*, 13175.
- (59) For examples of radical-mediated C–C coupling at nickel, see: (a) Csok, Z.; Vechorkin, O.; Harkins, S. B.; Scopelliti, R.; Hu, X. *J. Am. Chem. Soc.* **2008**, *130*, 8156. (b) Vechorkin, O.; Proust, V.; Hu, X. *J. Am. Chem. Soc.* **2009**, *131*, 9756. (c) Terao, J.; Watanabe, H.; Ikumi, A.; Kuniyasu, H.; Kambe, N. *J. Am. Chem. Soc.* **2002**, *124*, 4222. (d) Powell, D. A.; Fu, G. C. *J. Am. Chem. Soc.* **2004**, *126*, 7788.
- (60) Chirik, P. J.; Wieghardt, K. *Science* **2010**, *327*, 794.
- (61) The half arrows in these schemes are not intended to indicate outer-sphere electron transfer but rather the flow of electrons accompanying atom abstraction reactions.
- (62) A C–N bond length of 1.415(4) Å has been reported for an iminepyridine ligand side-on coordinated to a formally rhodium(I–) complex: Tejel, C.; Ciriano, M. A.; Del Río, M. P.; Van den Bruele, F.; Hettterscheid, D. G. H.; Tschlis i Spithas, N.; De Bruin, B. *J. Am. Chem. Soc.* **2008**, *130*, 5844.
- (63) Scott, J.; Gambarotta, S.; Korobkov, I. *Can. J. Chem.* **2005**, *83*, 279.
- (64) Cámpora, J.; Cartes, M. Á.; Rodríguez-Delgado, A.; Naz, A. M.; Palma, P.; Pérez, C. M. *Inorg. Chem.* **2009**, *48*, 3679.
- (65) Britovsek, G. J. P.; Gibson, V. C.; Kimberley, B. S.; Maddox, P. J.; McTavish, S. J.; Solan, G. A.; White, A. J. P.; Williams, D. J. *Chem. Commun.* **1998**, 849.
- (66) Activation of the LCoCl_2 catalyst precursor involves “noninnocent” cobalt(I) complexes,^{35,36} but the actual active species in polymerization is likely to contain cobalt(II) or cobalt(III) and an innocent DIMPY ligand.
- (67) Ligand oxidation may also be connected to electron transfer. See, e.g., ref 43 and the following: (a) Tejel, C.; Ciriano, M. A.; Del Río, M. P.; Hettterscheid, D. G. H.; Tschlis i Spithas, N.; Smits, J. M. M.; De Bruin, B. *Chem.—Eur. J.* **2008**, *14*, 10932. (b) Tejel, C.; Del Río, M. P.;

Ciriano, M. A.; Reijerse, E. J.; Hartl, F.; Zálaiš, S.; Hettler, D. G. H.; Tschlis i Spithas, N.; De Bruin, B. *Chem.—Eur. J.* **2009**, *15*, 11878.

(68) Blessing, R. *Acta Crystallogr.* **1995**, *A51*, 33.

(69) Sheldrick, G. M. *Acta Crystallogr.* **2008**, *A64*, 112.

(70) Ahlrichs, R.; Bär, M.; Baron, H.-P.; Bauernschmitt, R.; Böcker, S.; Ehrig, M.; Eichkorn, K.; Elliott, S.; Furche, F.; Haase, F.; Häser, M.; Hättig, C.; Horn, H.; Huber, C.; Huniar, U.; Kattannek, M.; Köhn, A.; Kölmel, C.; Kollwitz, M.; May, K.; Ochsenfeld, C.; Ohm, H.; Schäfer, A.; Schneider, U.; Treutler, O.; Tsereteli, K.; Unterreiner, B.; Von Arnim, M.; Weigend, F.; Weis, P.; Weiss, H. *Turbomole*, version 5; Theoretical Chemistry Group, University of Karlsruhe: Karlsruhe, Germany, 2002.

(71) Treutler, O.; Ahlrichs, R. *J. Chem. Phys.* **1995**, *102*, 346.

(72) Schäfer, A.; Horn, H.; Ahlrichs, R. *J. Chem. Phys.* **1992**, *97*, 2571.

(73) All *Turbomole* calculations were performed with the functional “b3-lyp” of that package, which is similar to (but not identical with) the Gaussian “B3LYP” functional.

(74) Lee, C.; Yang, W.; Parr, R. G. *Phys. Rev. B* **1988**, *37*, 785.

(75) Becke, A. D. *J. Chem. Phys.* **1993**, *98*, 1372.

(76) Becke, A. D. *J. Chem. Phys.* **1993**, *98*, 5648.

(77) PQS, version 2.4; Parallel Quantum Solutions: Fayetteville, AR, 2001 (the Baker optimizer is available separately from Parallel Quantum Solutions upon request).

(78) Baker, J. J. *Comput. Chem.* **1986**, *7*, 385.